

A Tikhonov Regularisation Approach to the Numerical Solution of Pipe Flows

NADANIELA EGIDI, JOSEPHIN GIACOMINI, PIERLUIGI MAPONI

School of Science and Technology - Mathematics Division,
University of Camerino,
Via Madonna delle Carceri 9, 62032 Camerino,
ITALY

Abstract: - Pipe flow problems deal with flows within tubes and are studied through Fluid Dynamics models. When considering pipe flow problems, turbulence often needs to be taken into account. Unfortunately, turbulence gives rise to difficulties in the computation of the approximated solution to such pipe flow problems, due to ill-conditioning. We propose an original stabilisation strategy based on Tikhonov regularisation for ill-posed problems. Some analytical insights on the applicability of this strategy are given, and its effectiveness is shown by a numerical experiment where the results of the proposed method are compared with the ones of a well-known solving strategy and an empirical solution for the axial velocity.

Key-Words: - Turbulent pipe flows, Navier-Stokes equations, ill-conditioning, Tikhonov regularisation, Numerical Solution.

Received: July 19, 2024. Revised: November 9, 2024. Accepted: December 11, 2024. Published: February 10, 2025.

1 Introduction

Pipe flows are internal fluid flows occurring inside pipes. This is a relevant branch of Fluid Dynamics, characterised by complex phenomena that sometimes are even not fully understood both from analytical and numerical point of view. Challenging pipe flow problems from real world applications are usually characterised by other difficulties, such as multiphase flows, [1], [2], turbulent flows [3], [4], [5], flows with cavitation [6], [7], [8], pulsatile flows, [9], [10], [11], transient flows [12], [13], non-Newtonian flows [2], [14]. These problems normally require numerical procedures that are properly refined depending on the characteristics of the problem itself. The interest in pipe flows studies is due to their connection to relevant real-life applications. For instance, the transportation of goods or material through a pipe is referred to as pipeline transport. Pipelines are employed for crude and refined petroleum, fuels (oil, natural gas and biofuels), liquid foods, sewage and slurry. Pipelines are also useful for the transport of drinking or irrigation water over large distances. In district heating systems, heated water or pressurised hot water or more rarely steam are delivered into insulated pipes. An important issue correlated to pipeline transportation is the internal and external corrosion due to the transported material, external agents and biofouling, which lead to pipe damages and consequently dangerous accidents or fatalities. Hence, the interest in preventing and mitigating corrosion is interdisciplinary and involves many fields such as Fluid Dynamics, Chemistry and Biology, [15], [16],

[17], [18]. Another important application of pipe flows is the study of the human cardiovascular system. Such system is made of pipes with multiple branches in which a complex non-Newtonian fluid, i.e., the blood, circulates. The blood vessels are living organs sensitive to blood cells, thus their compliance impacts on the hemodynamic conditions and vice-versa. For instance, normal arterial flow is laminar, with secondary flows generated at curves and branches, [9]. The study of blood flow is challenging from a theoretical point of view, because it involves pulsatile flows at the edge of turbulence. Moreover, numerical simulations of hemodynamics in the blood vessel can yield an accurate understanding of this kind of flow, which means the possibility to develop tools for early prediction and diagnosis of hemodynamic diseases, [2], [19], [20]. Another important application of pipe flows is heat exchangers. They are widely used in space heating and cooling, refrigeration, power stations, chemical plants and oil refineries. Due to the transition to a green and renewable energy system in the last decades, increasing attention has been paid to geothermal heat exchangers addressed to heat and cool spaces. In particular, the fluid flow into the single device and the relative heat exchange with the surrounding ground have been studied both numerically, [3], and experimentally, [21], [22], as well as geothermal fields with several devices have been investigated in terms of optimal performance in the long term, [23], [24], [25].

Pipe flow problems arising from real-world applications often deal with turbulence, which

is hard to address both from a theoretical and a computational point of view. A turbulent flow is still fully described by the Navier-Stokes equations, but their numerical solution requires high computational costs that are usually concretely impractical. Thus specific models are usually considered for the approximation of such turbulent flows. The classical computational models can be gathered into three kinds: Statistical Turbulence Modellings (STM), Large Eddy Simulations (LES), Direct Numerical Simulations (DNS). The STM approach, [26], makes the important phenomenological features of turbulent flows accessible by describing only the flow mean behaviour in such a way that the energy effects are preserved. The resulting system of equations is usually referred to as Reynolds Averaged Navier-Stokes (RANS). The LES approach, [26], fully solves the relevant large turbulent scales whereas models the small isotropic scales. Therefore, LES approach is usually more accurate and of wider applicability, though computationally more expensive than the RANS approach. An interesting comparison between the performance of RANS and LES turbulent models is provided in [27], for flows through rough pipes. Finally, the DNS approach, [28], [29], computes the numerical solution of the Navier-Stokes equations without the need for any additional turbulence model. Thus it provides a complete analysis of the flow, even if the corresponding approximation schemes are usually computationally demanding when applied to real-world problems.

The use of the DNS approach not only requires the availability of high-performance computational resources but often leads to difficulties in the computation of the solution, because of instability issues, [30], [31], [32]. Hence, stabilisation strategies should be applied to the discretised problem. In this paper, the DNS approach is applied to a pipe flow problem arising from the efficiency analysis of geothermal heat exchangers. In particular, the unsteady Navier-Stokes equations for a viscous, incompressible and Newtonian fluid are considered and discretised in space by means of the Galerkin finite element method and in time by an implicit finite difference scheme, [3]. The resulting system shows instability issues that cause an initial blow-up of the solution and consequently, the direct computation becomes unreliable. To overcome this difficulty, we propose a stabilisation strategy based on the Tikhonov regularisation. The Tikhonov regularisation usually deals with ill-posed problems in the sense of Hadamard, that is no solution exists, or at least one solution exists but it is not unique, or the solution exists and is unique, but does not continuously depend on the data, namely the initial and boundary

conditions. This latter case corresponds to unstable solutions, meaning that a small perturbation of initial-boundary data gives rise to an arbitrarily large perturbation of the solution at some point of the domain at a finite distance from the boundaries. This fact is of primary interest in the study of ill-posed problems, [33]. The typical example of an ill-posed problem is given by a Fredholm integral equation of the first kind, where the compact operator has singular values converging to zero. Such ill-posedness has consequences in the numerical treatment of the problem since classical discretisation methods usually end up in ill-conditioned problems. To overcome this instability issue, regularisation methods are applied and a stable approximate solution of ill-posed problems is obtained. The Tikhonov regularisation is based on a simple stabilisation scheme: given an equation for a compact linear and injective operator \mathcal{A} , the inverse of this operator is substituted with $(\alpha\mathcal{I} + \mathcal{A}^*\mathcal{A})^{-1}\mathcal{A}^*$, where $\alpha > 0$ is a proper parameter, \mathcal{I} is the identity operator and \mathcal{A}^* is the adjoint operator of \mathcal{A} . In this paper, a similar Tikhonov scheme is used, with \mathcal{A} equal to the Navier-Stokes operator. The effectiveness of this strategy is numerically proven by showing comparisons with a well-known empirical turbulent profile and OpenFOAM results. Finally, such a regularisation problem is part of an applied scenario of broad interest. In fact, it is driven by a clear applied aim which is the optimisation of a single geothermal exchanger, which in turn paves the way to the optimisation of a geothermal field with several devices. Naturally, the final goal of such optimisation processes is to provide an efficiency study of a renewable energy system with wide applicability. Nevertheless, the applicability of such a technique is not limited to the geothermal case but it has a direct impact on all the real-world problems that can be formalised as forced-convective problems for Newtonian fluids. Moreover, the context of applicability can be even greater with proper adjustments, including for instance large-scale pipeline transport systems or the cardiovascular system, where a non-Newtonian fluid and the interaction between blood and tissue must be considered.

The paper has the following structure. In Section 2, the analytical formulation and the considered numerical approximation of a pipe flow problem are described. In Section 3, the stabilisation strategy for an effective computation of the solution is introduced. In Section 4, the numerical results of the proposed solving strategy are shown and compared with empirical results and results obtained with different numerical techniques. Finally, in Section 5, some conclusions and future developments are

provided.

2 The'Ripe'How'Problem

We describe the mathematical formulation of the fluid flow problem in a pipe, which is given by the unsteady Navier-Stokes equations for viscous, incompressible and Newtonian fluids. The discretisation scheme is obtained by the Galerkin finite element method, [34], for the space variable, while temporal discretisation is based on a finite difference method. In Section 2.1, the mathematical model for the fluid flow is described; in Section 2.2, the discretisation scheme is derived and the resulting linear system is shown.

2.1 The'Formulation of the'How'Problem

The mathematical formulation of the flow problem through a three-dimensional region Ω is given in detail, then is applied in case Ω is a pipe. Let $\Omega \subset \mathbb{R}^3$ be the bounded open set, that in the following will be the mathematical representation of the pipe. Let $\mathbf{x} = (x_1, x_2, x_3)^T \in \Omega$ be the spatial variable, $t \in [0, \bar{t}]$ be the time variable and $\bar{t} > 0$ be the time of the flow observation; let $\mathbf{u}(\mathbf{x}, t) = (u_1(\mathbf{x}, t), u_2(\mathbf{x}, t), u_3(\mathbf{x}, t))^T \in \mathbb{R}^3$ be the fluid velocity and $P(\mathbf{x}, t)$ the ratio between the pressure and the density of the fluid (henceforth we refer to it simply as the pressure of the fluid). These functions are related through the well-known Navier-Stokes equations:

$$\begin{aligned} \frac{\partial \mathbf{u}}{\partial t}(\mathbf{x}, t) - \frac{1}{Re} \Delta \mathbf{u}(\mathbf{x}, t) + (\mathbf{u} \cdot \nabla) \mathbf{u}(\mathbf{x}, t) + \\ + \nabla P(\mathbf{x}, t) = 0, \quad \mathbf{x} \in \Omega, 0 < t < \bar{t}, \quad (1) \\ \nabla \cdot \mathbf{u}(\mathbf{x}, t) = 0, \quad \mathbf{x} \in \Omega, 0 < t < \bar{t}, \quad (2) \end{aligned}$$

where ∇ denotes the gradient operator and Δ the laplacian operator, $Re = \rho U D / \mu$ is the Reynolds number, ρ, μ are the density and the viscosity, respectively, of the carrier fluid which is supposed incompressible, and U, D are the flow characteristic velocity and the pipe diameter, respectively. In particular, Eq. (1) derives from the momentum balance and Eq. (2) is the continuity equation for the mass balance, see, [34], [35], for a detailed presentation of these equations.

For its solution, problem (1),(2) must be equipped with suitable boundary and initial conditions. Indeed, the pressure $P(\mathbf{x}, t)$ can be determined up to a constant because it appears as a Lagrangian multiplier associated to the divergence-free constraint (2), see, [34], for details. When Ω is a pipe, let Γ be the boundary of Ω , we assume it is divided into three parts, as in Fig. 1: the inlet face Γ_{in} , where the fluid enters the pipe, the outlet face Γ_{out} , where the fluid exits, and the wall surface Γ_w , which is indeed the pipe wall. More clearly, $\Gamma_{in}, \Gamma_{out}$ and Γ_w have empty

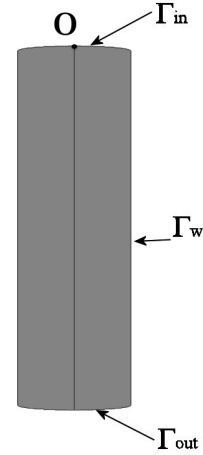


Fig. 1: The pipe with the relevant boundary components. The picture is not scaled uniformly along different directions

two by two intersection and $\Gamma = \Gamma_{in} \cup \Gamma_{out} \cup \Gamma_w$, moreover the closure of Ω is $\bar{\Omega} = \Omega \cup \Gamma$. The following conditions are considered:

$$\mathbf{u}(\mathbf{x}, t) = \beta(\mathbf{x}), \quad \mathbf{x} \in \Gamma_{in}, 0 < t \leq \bar{t}, \quad (3)$$

$$\frac{1}{Re} \frac{\partial \mathbf{u}}{\partial \hat{n}}(\mathbf{x}, t) - P(\mathbf{x}, t) \hat{n} = \mathbf{0}, \quad \mathbf{x} \in \Gamma_{out}, 0 < t \leq \bar{t}, \quad (4)$$

$$\mathbf{u}(\mathbf{x}, t) = \mathbf{0}, \quad \mathbf{x} \in \Gamma_w, 0 < t \leq \bar{t}, \quad (5)$$

$$\mathbf{u}(\mathbf{x}, 0) = \alpha(\mathbf{x}), \quad \mathbf{x} \in \Omega \cup \Gamma, \quad (6)$$

where $\mathbf{0}$ is the three-dimensional null vector, \hat{n} is the outward unit normal with respect to the boundary Γ , α is the initial velocity and satisfies the compatibility condition on the boundary, β is the inlet velocity. Equations (1)-(6) define the flow problem considered in the following of this paper.

2.2 The'Pumerical'Uolution of the'How'Problem

To solve the flow problem formalised in (1)-(6), it is necessary to discretise it. Here we propose an approximation scheme based on the Galerkin method with a finite element basis. In particular, the domain $\bar{\Omega}$ is discretised by a tetrahedral mesh. The set $V = \{\mathbf{v}_1, \mathbf{v}_2, \dots, \mathbf{v}_{N_V}\}$ of the nodes of this mesh is composed by the four vertices of each tetrahedron and the six middle points of its edges. We denote with $H = \{h_1, h_2, \dots, h_{N_H}\}$ the set of the indices of interior or outlet nodes, so $\mathbf{v}_h \in \Omega \cup \Gamma_{out}, h \in H$; $B = \{b_1, b_2, \dots, b_{N_B}\}$ the set of the indices of nodes in $\Gamma_{in} \cup \Gamma_w$; $G = \{g_1, g_2, \dots, g_{N_G}\}$ the set of the indices

of the vertices in $\Omega \cup \Gamma_{\text{out}}$; $C = \{c_1, c_2, \dots, c_{N_C}\}$ the set of the indices of the vertices in $\Gamma_{\text{in}} \cup \Gamma_w$. We note that $N_N = N_H + N_B$ and $J = H \cup B = \{1, 2, \dots, N_N\}$ is the set of the indices of all nodes in Ω ; finally, $K = G \cup C$ is the set of the indices of all the vertices in Ω and its cardinality is $N_K = N_G + N_C$.

The detailed procedure for the discretisation of problem (1)-(6) is reported in Appendix A.

For later convenience, we write here the discretised system (24),(25), obtained in Appendix A, in a compact matrix form. In particular, given $N_t > 0$, $\Delta t = \bar{t}/N_t$, and $t_n = n\Delta t$, $n = 0, 1, \dots, N_t$, then for $n = 0, 1, \dots, N_t - 1$

$$\left\{ \begin{array}{l} (M^H + S^H + N^H(t_n)) \mathbf{u}_i^H(t_{n+1}) + \\ + (L_i^H)^T \mathbf{P}(t_{n+1}) = \\ - (M^B + S^B + N^B(t_n)) \mathbf{u}_i^B(t_{n+1}) + \\ + M \mathbf{u}_i(t_n), \quad i = 1, 2, 3 \quad (7) \\ L_1^H \mathbf{u}_1^H(t_{n+1}) + L_2^H \mathbf{u}_2^H(t_{n+1}) + \\ + L_3^H \mathbf{u}_3^H(t_{n+1}) = \\ - (L_1^B \mathbf{u}_1^B(t_{n+1}) + L_2^B \mathbf{u}_2^B(t_{n+1}) + \\ + L_3^B \mathbf{u}_3^B(t_{n+1})), \quad (8) \end{array} \right.$$

where all the matrices $M, S, N(t_n), L_i, i = 1, 2, 3$, are defined in formulas (30)-(33) of Appendix A, the unknown vectors at time t_{n+1} , $\mathbf{u}_i^H(t_{n+1}), i = 1, 2, 3$, $\mathbf{P}(t_{n+1})$ are defined in formulas (26),(27), respectively, the already computed vectors at time t_n $\mathbf{u}_i(t_n), i = 1, 2, 3$, and the known vectors on the boundary at time t_{n+1} $\mathbf{u}_i^B(t_{n+1}), i = 1, 2, 3$, occurring in the known terms are defined in formulas (28),(29), respectively.

We denote by A_n the coefficient matrix of (7),(8), that is

$$A_n = \begin{pmatrix} Q_n^H & 0 & 0 & (L_1^H)^T \\ 0 & Q_n^H & 0 & (L_2^H)^T \\ 0 & 0 & Q_n^H & (L_3^H)^T \\ L_1^H & L_2^H & L_3^H & 0 \end{pmatrix}, \quad (9)$$

where $Q_n^H = M^H + S^H + N^H(t_n)$. Then the system to solve at each time step is

$$A_n \mathbf{x}_{n+1} = \mathbf{b}, \quad (10)$$

where

$$\mathbf{x}_{n+1} = \begin{pmatrix} \mathbf{u}_1^H(t_{n+1}) \\ \mathbf{u}_2^H(t_{n+1}) \\ \mathbf{u}_3^H(t_{n+1}) \\ \mathbf{P}(t_{n+1}) \end{pmatrix}$$

is the unknown vector and \mathbf{b} is the known vector made of the right-hand-side of system (7),(8). System (10) represents the discretisation scheme of

problem (1)-(6), and its solution defines the numerical approximation of the velocity field and the pressure field. We observe that this system is based on the linearisation (23), so the corresponding velocity solution may be a rough approximation of the real velocity field. A fixed-point iterative strategy usually provides a satisfactory refinement of the solution at each time step, consisting in a repeated solution of the linear system until a stop criterium is satisfied. More precisely, let $\mathbf{x}_{n+1,0}$ be the solution of

$$A_n \mathbf{x}_{n+1,0} = \mathbf{b}.$$

This solution is used as initial guess of the following recursive procedure: from $\mathbf{x}_{n+1,\nu-1}, \nu = 1, 2, \dots$, the matrix $A_{n+1,\nu-1}$ is computed by using $\mathbf{u}_i^H(t_{n+1,\nu-1})$ in the construction of the matrix N^H (see Equation (32)), and $\mathbf{x}_{n+1,\nu}$ is computed as solution of

$$A_{n+1,\nu-1} \mathbf{x}_{n+1,\nu} = \mathbf{b}.$$

This procedure terminates when the stop criterion $\|\mathbf{x}_{n+1,\nu} - \mathbf{x}_{n+1,\nu-1}\|_2 < \varepsilon$ is verified for a prescribed tolerance $\varepsilon > 0$, where $\|\cdot\|_2$ is the Euclidean norm. However, the solution of this system is not a trivial task, in fact, the corresponding coefficient matrix is not positive-definite, not symmetric, it has a high sparsity pattern and a zero block on the main diagonal corresponding to Equation (8); moreover, the system is ill-conditioned for high Reynolds numbers. Therefore the computation of the solution requires the usage of stabilisation techniques, especially when turbulent flows are considered.

3 The 'Utabilisation' Utrategy

We propose to compute the solution of linear systems (10) by using a stabilisation technique based on the Tikhonov regularisation. This is a regularisation method commonly used for ill-posed problems in the sense of Hadamard. The flow problem under consideration is based on the Navier-Stokes operator, which has a quite different nature with respect to problems for the compact integral operators usually solved by the Tikhonov regularisation. Nevertheless, turbulence strongly influences the dynamic of the flow and creates instability in the problem, as divergent solutions, which can be seen as a kind of ill-posedness. In fact, when turbulence increases, the Reynolds number is high, so the second-order diffusive part of Equation (1) is dominated by the first-order advective part. It follows the difficulty in the prescription of the boundary conditions when the first order term dominates. Despite the relation between turbulent flows and ill-posedness deserves further investigations, in the limit $Re \rightarrow \infty$, hence in

a very high turbulent state, problem (1)-(6) becomes ill-posed because the given boundary conditions are inappropriate and should be prescribed in accordance to the nature of the resulting advective problem, [36]. From a numerical point of view, turbulence has an impact on the conditioning of the discretised Navier-Stokes equations, in particular, problem (10) is ill-conditioned when a fully turbulent state arises.

We illustrate the Tikhonov regularisation on problem (1),(2) by means of the corresponding discretised problem (10), where the flow problem is already reduced to a finite-dimensional problem. The modified Tikhonov functional that we propose as stabilisation strategy for solving problem (10) is

$$\|A_n \mathbf{x} - \mathbf{b}\|^2 + \|\Lambda_1 J_1 \mathbf{x}\|^2 + \|\Lambda_2 J_2 \mathbf{x}\|^2, \quad (11)$$

where $\Lambda_1 J_1$ and/or $\Lambda_2 J_2$ are non-singular and

$$J_1 = \begin{pmatrix} M^H & 0 & 0 & 0 \\ 0 & M^H & 0 & 0 \\ 0 & 0 & M^H & 0 \\ 0 & 0 & 0 & I \end{pmatrix}, \quad (12)$$

$$J_2 = \begin{pmatrix} S^H & 0 & 0 & 0 \\ 0 & S^H & 0 & 0 \\ 0 & 0 & S^H & 0 \\ 0 & 0 & 0 & 0 \end{pmatrix}, \quad (13)$$

$$\Lambda_1 = \begin{pmatrix} D_1^1 & 0 & 0 & 0 \\ 0 & D_1^2 & 0 & 0 \\ 0 & 0 & D_1^3 & 0 \\ 0 & 0 & 0 & D_1^4 \end{pmatrix}, \quad (14)$$

$$\Lambda_2 = \begin{pmatrix} D_2^1 & 0 & 0 & 0 \\ 0 & D_2^2 & 0 & 0 \\ 0 & 0 & D_2^3 & 0 \\ 0 & 0 & 0 & D_2^4 \end{pmatrix}, \quad (15)$$

with $D_1^i, D_2^i, i = 1, 2, 3, 4$, diagonal matrices containing the non-negative Tikhonov parameters and I identity matrix of order N_K . The functional in (11) differs from the common Tikhonov functional, [33], for the presence of two distinct Tikhonov matrices, J_1 and J_2 , and consequently, for the presence of multiple regularisation parameters that constitutes the diagonal matrices Λ_1 and Λ_2 . Such parameters differ varying the diagonal block and so the velocity components as well as pressure have an ad-hoc stabilisation. From the Tikhonov regularisation theory, finding the minimum of the Tikhonov functional is equivalent to finding the solution of a proper regularisation scheme, [33]. In particular, the following theorem holds.

Theorem 1. *Let A be the matrix in (9) and let $J_i, \Lambda_i, i = 1, 2$, matrices as in (12)-(15). Then for each $\mathbf{b} \in \mathbb{R}^{N_H+N_K}$ there exists a unique $\bar{\mathbf{x}} \in \mathbb{R}^{N_H+N_K}$ such that*

$$\|A\bar{\mathbf{x}} - \mathbf{b}\|^2 + \|\Lambda_1 J_1 \bar{\mathbf{x}}\|^2 + \|\Lambda_2 J_2 \bar{\mathbf{x}}\|^2 =$$

$$= \inf_{\mathbf{x}} (\|A\mathbf{x} - \mathbf{b}\|^2 + \|\Lambda_1 J_1 \mathbf{x}\|^2 + \|\Lambda_2 J_2 \mathbf{x}\|^2).$$

The minimum point $\bar{\mathbf{x}}$ is given by the unique solution of equation

$$\left(A^T A + J_1^T (\Lambda_1)^2 J_1 + J_2^T (\Lambda_2)^2 J_2 \right) \mathbf{x} = A^T \mathbf{b}. \quad (16)$$

Proof. See Appendix B. \square

We note that, for the proposed Tikhonov regularisation, the regularised solution of (16) converges to the original solution of Equation (10), as the regularisation parameters in Λ_1, Λ_2 tend to zero. Considering also that the regularisation is done at each time step, this implies that the convergence of the Galerkin numerical scheme remains unaffected. The choice of the optimal regularisation parameters in Λ_1, Λ_2 is a critical phase and in general it can be made by the discrepancy principle, [33]. Here, we consider an easier approach. Roughly speaking, they must be chosen small enough to obtain only a slightly perturbed solution of the normal equations of (10) and sufficiently large to obtain a well-conditioned linear system. In other words, both accuracy and stability of the solution must be taken into account: the accuracy is conveyed by small regularisation parameters, the stability instead by large ones. The optimal choice is the one that makes a compromise between accuracy and stability, meaning that both the residual and the regularised solution are minimised, as stated in Theorem 1. As usual in regularisation strategies, the parameters are selected by a trial-and-error procedure or by using discrepancy principles, [37], [38], in accordance with some a-priori information on data error and on the solution \mathbf{x}_n . So, in this paper we show that a proper choice of the parameters can effectively stabilise the computation of turbulent flows. Future works have to define efficient strategies for choosing optimal parameters. Finally, it is worth noting that linear system (16) has also favourable computational properties. In fact, the action of this matrix can be computed efficiently by using the sparsity of the original coefficient matrix (9). Besides, such coefficient matrix is also positive-definite and symmetric thus the solution of system (16) can take advantage of algebraic solvers for symmetric positive-definite matrices.

4 Numerical Results

We show some results obtained by the proposed method applied to turbulent pipe flows, considering the real case of a geothermal exchanger. In Section 4.1, details about the setup of the numerical simulations are given. In Section 4.2, the results of the proposed stabilisation strategy are shown and compared with heuristic results on turbulent

pipe flows and a solving strategy used by the well-known Computational Fluid Dynamics software OpenFOAM.

4.1 Numerical Framework

The domain Ω corresponds to a pipe with diameter $D = 0.032$ m and length $L = 0.314$ m. The corresponding discretised domain consists in 11761 tetrahedral elements and 2976 vertices, with mean element side of $5.9 \cdot 10^{-3}$. Over this mesh, we choose the following two finite element bases $\psi_j, j \in J$, and $\phi_k, k \in K$, for the velocity \mathbf{u} and the pressure P , respectively: ψ_j is the unique quadratic function on each tetrahedron such that $\psi_j(\mathbf{v}_l) = \delta_{j,l}$ for all $j, l \in J$, where $\delta_{\cdot, \cdot}$ is the Kronecker symbol; ϕ_k is the unique linear function on each tetrahedron such that $\phi_k(\mathbf{v}_l) = \delta_{k,l}$ for all $k, l \in K$. Note that these functions are continuous in Ω and continuously differentiable in each tetrahedron, see, [39], for a detailed description of these bases and their construction. Moreover, this choice, consisting in a basis for pressure having at least one degree less than the one for the velocity, guarantees the Ladyzhenskaya-Brezzi-Babuška condition, which can be seen as a stability criterion for the discretisation scheme, [39].

In problem (1)-(6), we suppose a null initial inner fluid velocity, $\alpha(\mathbf{x}) = \mathbf{0}$. Instead, in the following we simulate two cases, for which the inlet boundary condition prescribes a constant and uniform fluid velocity: in the first case $\beta(\mathbf{x}) = (0, 0, 1)^T$; in the second case $\beta(\mathbf{x}) = (0, 0, 5)^T$. In addition, the carrier fluid is water and its characteristics are considered at a reference temperature of about 300 K, [40]: the density $\rho = 9.9651 \cdot 10^2$ kg/m³ and the viscosity $\mu = 8.5384 \cdot 10^{-4}$ kg/m·s. Thus, the Reynolds number for each considered case is: 1. $3.7 \cdot 10^4$, 2. $1.9 \cdot 10^5$.

Regarding the numerical parameters, we consider: a time step $\Delta t = 10^{-3}$ and the number of time steps $N_t = 300$. The solution of linear system (16) is computed by Gaussian elimination with partial pivoting, and tolerance of the fixed-point iterative is $\varepsilon = 10^{-5}$. In particular, the chosen Tikhonov parameters for the first considered case, $\beta(\mathbf{x}) = (0, 0, 1)^T$, are

$$\begin{aligned} (D_1^1)_{h,h}^2 &= (D_1^2)_{h,h}^2 = 10^{-8}, \\ (D_1^3)_{h,h}^2 &= 10^{-10} \exp\left(-\frac{\|\mathbf{v}_h - \mathbf{c}\|_2}{0.003}\right) + 10^{-13}, \\ (D_1^4)_{h,h}^2 &= 10^{-13}, \\ (D_2^i)_{h,h}^2 &= 10^{-6}, \quad i = 1, 2, 3, 4, \end{aligned}$$

for the second considered case, $\beta(\mathbf{x}) = (0, 0, 5)^T$, are

$$\begin{aligned} (D_1^1)_{h,h}^2 &= (D_1^2)_{h,h}^2 = 10^{-7}, \\ (D_1^3)_{h,h}^2 &= 10^{-11} \exp\left(-\frac{\|\mathbf{v}_h - \mathbf{c}\|_2}{0.003}\right) + 10^{-12}, \\ (D_1^4)_{h,h}^2 &= 10^{-13}, \\ (D_2^i)_{h,h}^2 &= 10^{-7}, \quad i = 1, 2, 3, 4, \end{aligned}$$

for $h \in H$, where \mathbf{c} is the centre of the cross section to which the node \mathbf{v}_h belongs. The rationale behind this choice of the regularisation parameters is the following. For the action on the mass matrix M^H , the non axial components of the velocity must be regularised more severely with respect to the axial component, in fact, on average the dominant velocity component must be u_3 , even in turbulent state; besides, the regularisation for u_3 is greater on the pipe axis and very small at the pipe boundary. For the action on the diffusive matrix S^H , the regularisation parameters must be larger to prevent the velocity gradient from blowing up. However, a formal analysis for the optimal choice of the regularisation parameters should be performed in a further development.

The proposed solving strategy is compared with another classical strategy that we briefly describe. In particular, we consider the pipe flow problem (1)-(6) endowed with the RANS equations as turbulence model. This is a classical model to handle turbulence belonging to the STM approach, [26], where the instantaneous velocity field is decomposed into the mean value and a fluctuating term. Then, the resulting turbulent model is discretised by the collocated cell-centred finite volume method, [36]. The solving strategy relies on the PISO algorithm, [41]. This is a segregated solver, meaning that the velocity and pressure computation are decoupled. In more detail, the main steps of this solving strategy can be summed up as follows: the momentum equation is solved first, then the mass fluxes at cells faces are computed and the pressure equation is solved. Thus, the mass fluxes are corrected and the new velocity field is calculated by exploiting the computed pressure field. All these steps are repeated as many times as prescribed by the user.

Finally, we report an analytical expression for the velocity profile in turbulent pipe flows that will be used as reference for the numerical results. Such empirical law is based on experimental observations and describes the average profile of the axial velocity along the radial direction on a cross section of the pipe. It is the well-known one-seventh power

law, [42]:

$$u(\mathbf{x}) = u_{\max} \left(\frac{r - \|\mathbf{x} - \mathbf{c}\|_2}{r} \right)^{1/7}, \quad (17)$$

where r is the pipe radius, \mathbf{c} is the pipe centre and u_{\max} is the maximal velocity at the centre of the pipe. In this case of study, $u_{\max} = 8/7U$, where U is the mean velocity of the profile, calculated by the mean-value Theorem, and it must coincide with the mean velocity of the inlet profile along the z -direction. We remark that the one-seventh power law fails to be accurate at the centre of the pipe and in the viscous sublayer, namely the very thin layer next to the wall where viscous effects are dominant, but it describes quite precisely the turbulent flow in the most portion of the section.

4.2 Results and Discussion

We show the numerical results obtained by the stabilisation strategy proposed in (16) compared with the numerical results obtained by OpenFOAM, and at the same time we compare both to the reference profile given by the empirical law in (17).

Figure 2 reports the results for the case 1. at the last time step and along a radius of a cross section at half length of the pipe. In more detail, the blue line with circular markers shows the numerical results with the stabilisation strategy based on Tikhonov regularisation and averaged over points at the same distance from the centre; the red line with squared markers shows the empirical profile in (17); the green line with triangular markers shows the numerical results obtained with OpenFOAM. The three velocity profiles in Figure 2 are in great agreement near the centre of the pipe; for a distance from the pipe wall in the interval $(0.004, 0.01)$, approximately, the green profile is slightly better than the blue one with respect to the empirical solution (red profile); whereas, near the wall the blue profile tends to increase a bit faster than the green one and it does not show a linear trend. However, both the proposed stabilisation strategy and OpenFOAM give very similar results that closely follow the empirical profile except for the layer near the pipe wall, where the velocity shows a quick boost.

Figure 3 reports the results for the case 2. at the last time step and along a radius of a cross section at half length of the pipe. The same correspondence between colors and velocity profiles has been kept as before. Near the pipe wall, the blue profile is much nearer to the red empirical profile than the green one, moreover, the blue profile shows an initial boost of the velocity whereas the green profile has a linear and not steep slope. Then, moving towards the centre till the distance 0.012 from the wall, both

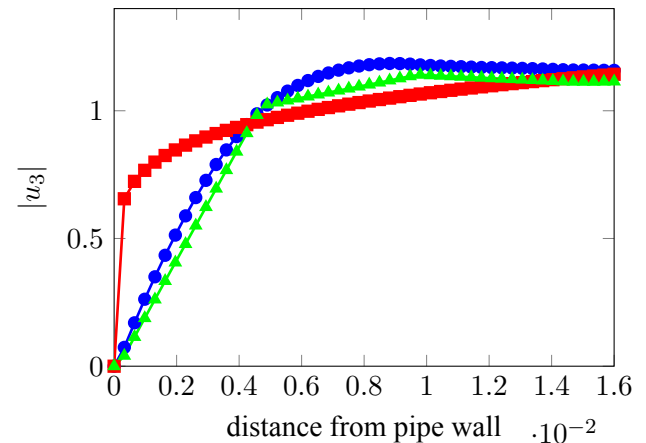


Fig. 2: Axial velocity profiles for the case 1

at the last time step and along a radius of a cross section at half length of the pipe, obtained by: the stabilisation strategy based on Tikhonov regularisation (blue line with circular markers), the empirical one-seventh power law (red line with squared markers), OpenFOAM (green line with triangular markers).

the blue and green profiles follow quite closely the red profile, except for a pick in the blue line. Near the centre, the blue profile goes farther from the red one. In general, the results from our stabilisation give a behaviour that best resembles the empirical law, and some picks appear due to the high turbulence; while the results from OpenFOAM seems unaffected by turbulence intensity, showing in fact the same behaviour in Fig. 2, Fig. 3 and the trend of the axial velocity near the wall is quite inaccurate.

5 Conclusions

The solution of the discretised Navier-Stokes problem in the presence of turbulence is quite challenging, especially when no turbulence models are exploited. This is due to unfavourable characteristics of the coefficient matrix and its oscillating eigenvalues for high Reynolds numbers. In this paper, we proposed a stabilisation strategy that is based on Tikhonov regularisation. We showed that this strategy works satisfactorily for a turbulent pipe flow problem in the real case of a geothermal exchanger, with two different flow velocities causing a high turbulent regime. The effectiveness of this strategy has been shown by a comparison with the solving strategy used in OpenFOAM, for turbulent flows, by using a reference velocity profile given by a commonly accepted heuristic law. In this initial exploration of the topic, we proposed numerical simulations concerning a rectilinear geothermal exchanger, due to data availability as well as the possibility to use a

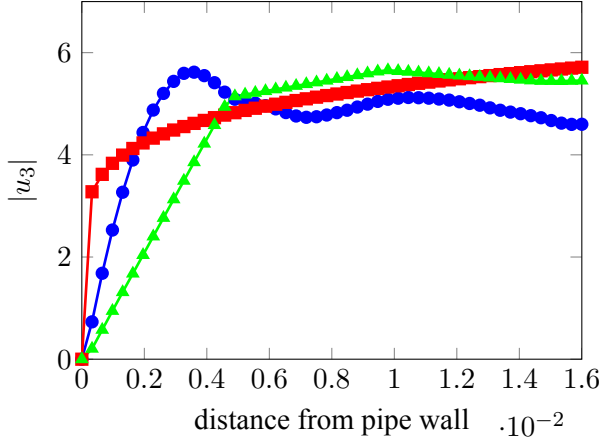


Fig. 3: Axial velocity profiles for the case 2

at the last time step and along a radius of a cross section at half length of the pipe, obtained by: the stabilisation strategy based on Tikhonov regularisation (blue line with circular markers), the empirical one-seventh power law (red line with squared markers), OpenFOAM (green line with triangular markers).

reference fully-developed velocity profile in turbulent state. Of course, this strategy can be applied to geothermal exchangers with a different geometry, preserving a similar effectiveness, since it is free from shape constraints. In addition, the scope of this study goes beyond the heat exchanger problem, because it could be applied to any real-world problem described by the Navier-Stokes equations, and even to hemodynamics in the cardiovascular system under proper adjustments.

The proposal of using the Tikhonov regularisation scheme for ill-posed problems as a stabilisation technique for a turbulent pipe flow problem is innovative. Thus, the relation between turbulence and ill-posedness must be investigated in more detail, and the effectiveness of the proposed method must be extensively assessed both analytically and numerically. Further developments of this work should consider testing the strategies against different mesh sizes, as well as devising a general strategy for choosing the regularisation parameters, by searching for a kind of normalization of the Tikhonov parameters depending on the inlet velocity and/or the mesh size. Finally, we would like to investigate the correlation between our method and artificial viscosity methods, [43], since in the proposed stabilisation scheme the matrix Λ_2 in (16) could be seen as a kind of artificial viscosity.

A The Discretisation of the Flow Problem

Let $W = H_0^1(\Omega)$ be the closure of $C_0^\infty(\Omega)$, i.e., the space of infinitely differentiable functions having compact support in Ω , with respect to the norm in $H^1(\Omega)$. Let $Q = L_0^2(\Omega)$ be the space of square integrable functions with null average, i.e., $L_0^2(\Omega) = \{q \in L^2(\Omega) : \int_\Omega q = 0\}$. Let $u_i \in H_0^1(\Omega)$, $i = 1, 2, 3$, and $P \in L_0^2(\Omega)$. We need to define the finite-dimensional spaces correspondent to these spaces, in order to apply the Galerkin discretisation to the problem (1)-(6). Let $h > 0$ and W_h, Q_h finite-dimensional subspaces of W, Q of dimension N_N, N_K , respectively. Furthermore, we assume that W_h and Q_h are compatible spaces, [34], that is their functions satisfy the compatibility (or Ladyzhenskaya-Babuška-Brezzi) condition. Let ψ_j , $j \in J$, be a basis of W_h and ϕ_k , $k \in K$, be a basis for Q_h . In particular, $\psi_j(\mathbf{v}_l) = \delta_{j,l}$ for all $j, l \in J$, and $\phi_k(\mathbf{v}_l) = \delta_{k,l}$ for all $k, l \in K$, thus ψ_j has compact support in the tetrahedra containing the node \mathbf{v}_j and ϕ_k has compact support in the tetrahedra containing the vertex \mathbf{v}_k . For each $t \in [0, \bar{t}]$, let $\tilde{\mathbf{u}}(\cdot, t) = (\tilde{u}_1(\cdot, t), \tilde{u}_2(\cdot, t), \tilde{u}_3(\cdot, t))^T$, with $\tilde{u}_i \in W_h$, $i = 1, 2, 3$, an approximation of $\mathbf{u}(\mathbf{x}, t)$ and $\tilde{p}(\cdot, t) \in Q_h$ an approximation of $P(\cdot, t)$, having the following forms:

$$\tilde{u}_i(\mathbf{x}, t) = \tilde{u}_{i,\partial}(\mathbf{x}, t) + \sum_{h \in H} u_i^h(t) \psi_h(\mathbf{x}), \quad i = 1, 2, 3, \quad (18)$$

$$\tilde{u}_{i,\partial}(\mathbf{x}, t) = \sum_{b \in B} u_i^b(t) \psi_b(\mathbf{x}), \quad i = 1, 2, 3, \quad (19)$$

$$\tilde{p}(\mathbf{x}, t) = \sum_{k \in K} P^k(t) \phi_k(\mathbf{x}), \quad (20)$$

where $\mathbf{x} \in \bar{\Omega}$, $0 \leq t \leq \bar{t}$, $u_i^b(t) = \beta_i(\mathbf{v}_b)$ when $b \in B$ and $\mathbf{v}_b \in \Gamma_{in}$, $u_i^b(t) = 0$ when $b \in B$ and $\mathbf{v}_b \in \Gamma_w$, whereas $u_i^h(t)$, $h \in H$, and $P^k(t)$, $k \in K$, are unknown coefficients.

The semi-discrete Galerkin approximation of problem (1),(2) reads:

$$\int_\Omega \left(\frac{\partial \tilde{\mathbf{u}}(\cdot, t)}{\partial t} - \frac{1}{Re} \Delta \tilde{\mathbf{u}}(\cdot, t) + (\tilde{\mathbf{u}}(\cdot, t) \cdot \nabla) \tilde{\mathbf{u}}(\cdot, t) + \nabla \tilde{p}(\cdot, t) \right) \psi_h d\mathbf{x} = 0, \quad h \in H, \quad (21)$$

$$\int_\Omega \nabla \cdot \tilde{\mathbf{u}}(\cdot, t) \phi_k d\mathbf{x} = 0, \quad k \in K, \quad (22)$$

where test functions ψ_h , $h \in H$, are used for the momentum equations and ϕ_k , $k \in K$ for the continuity equation. To obtain the full discretised

problem, Eq. (21) needs the discretisation of the time derivative and the linearisation procedure. Let $N_t > 0$ and $\Delta t = \bar{t}/N_t$ be the time step, let $t_n = n\Delta t$, $n = 0, 1, \dots, N_t$. We apply the time advancing by the finite difference method. In more detail, the $n + 1$ time step, system (21),(22) is evaluated at $t = t_{n+1}$ and the time derivative is approximated with a backward finite difference quotient, that is

$$\frac{\partial \tilde{\mathbf{u}}(\cdot, t_{n+1})}{\partial t} \approx \frac{\tilde{\mathbf{u}}(\cdot, t_{n+1}) - \tilde{\mathbf{u}}(\cdot, t_n)}{\Delta t},$$

providing a procedure resembling the implicit Euler scheme. The non linear term in Eq. (21) is linearised by means of the classical technique for Oseen problems:

$$(\tilde{\mathbf{u}}(\mathbf{x}, t_{n+1}) \cdot \nabla) \tilde{\mathbf{u}}(\mathbf{x}, t_{n+1}) \psi_h(\mathbf{x}) \approx (\tilde{\mathbf{u}}(\mathbf{x}, t_n) \cdot \nabla) \tilde{\mathbf{u}}(\mathbf{x}, t_{n+1}) \psi_h(\mathbf{x}). \quad (23)$$

The resulting algebraic form of problem (21),(22) is obtained by substituting formulas (18)-(20) in the integral equations, then we apply the Green's first identity to the Laplacian term and the divergence Theorem to the pressure gradient in Eq. (21). Hence, from the property $\psi_h(\mathbf{x}) = \phi_g(\mathbf{x}) = 0$, $\mathbf{x} \in \Gamma \setminus \Gamma_{\text{out}}$, $h \in H$, $g \in G$, and the boundary condition (4), a system of linear equations for the unknowns $u_i^h(t_{n+1})$, $h \in H$, and $P^k(t_{n+1})$, $k \in K$, is obtained for each $n = 0, 1, \dots, N_t - 1$,

$$\begin{aligned} & \sum_{l \in H} (M_{h,l} + S_{h,l} N_{h,l}(t_n)) u_i^l(t_{n+1}) + \\ & + \sum_{k \in K} (L_i^T)_{h,k} P^k(t_{n+1}) = \\ & - \sum_{b \in B} (M_{h,b} + S_{h,b} + N(t_n)_{h,b}) u_i^b(t_{n+1}) + \\ & + \sum_{j \in J} M_{h,j} u_i^j(t_n), \quad i = 1, 2, 3, \quad (24) \end{aligned}$$

$$\begin{aligned} & \sum_{i=1}^3 \sum_{l \in H} (L_i)_{k,l} u_i^l(t_{n+1}) = \\ & - \sum_{i=1}^3 \sum_{b \in B} (L_i)_{k,b} u_i^b(t_{n+1}), \quad (25) \end{aligned}$$

where the unknown vectors are

$$\mathbf{u}_i^H(t_n) = (u_i^{h_1}(t_n), \dots, u_i^{h_{N_H}}(t_n))^T, \quad (26)$$

$$\mathbf{P}(t_n) = (P^{k_1}(t_n), \dots, P^{k_{N_K}}(t_n))^T, \quad (27)$$

while the known term gathers the contribution of the previous time step and the Dirichlet boundary

conditions, and it is made of

$$\mathbf{u}_i(t_n) = (u_i^{h_1}(t_n), \dots, u_i^{h_{N_H}}(t_n), u_i^{b_1}(t_n), \dots, u_i^{b_{N_B}}(t_n))^T, \quad (28)$$

$$\mathbf{u}_i^B(t_n) = (u_i^{b_1}(t_n), \dots, u_i^{b_{N_B}}(t_n))^T. \quad (29)$$

In addition, the following matrices are defined for $h \in H$, $j \in J$, $k \in K$,

$$M_{h,j} = \frac{1}{\Delta t} \int_{\Omega} \psi_h \psi_j d\mathbf{x}, \quad M = (M^H, M^B), \quad (30)$$

$$S_{h,j} = \frac{1}{Re} \int_{\Omega} \nabla \psi_h \cdot \nabla \psi_j d\mathbf{x}, \quad S = (S^H, S^B), \quad (31)$$

$$\begin{aligned} N_{h,j}(t_n) &= \sum_{l \in J} \sum_{s=1}^3 u_s^l(t_n) \int_{\Omega} \frac{\partial \psi_j}{\partial x_s} \psi_h \psi_l d\mathbf{x}, \\ N(t_n) &= (N^H(t_n), N^B(t_n)), \quad (32) \end{aligned}$$

$$\begin{aligned} (L_i)_{k,j} &= - \int_{\Omega} \frac{\partial \psi_j}{\partial x_i} \phi_k d\mathbf{x}, \\ L_i &= (L_i^H, L_i^B), \quad i = 1, 2, 3. \quad (33) \end{aligned}$$

We note that, at the right-hand side of formulas (30)-(33) it is defined a column-partition of the corresponding matrix with respect to the two disjoint sets of indices H and B .

B Proof of Theorem 1

Proof. Adding and subtracting to each addendum of the Tikhonov functional (11) the action of the relative

matrix over the minimiser $\bar{\mathbf{x}}$, we obtain

$$\begin{aligned} & \|A\mathbf{x} - \mathbf{b}\|^2 + \|\Lambda_1 J_1 \mathbf{x}\|^2 + \|\Lambda_2 J_2 \mathbf{x}\|^2 \\ &= \|A\bar{\mathbf{x}} - \mathbf{b}\|^2 + \|\Lambda_1 J_1 \bar{\mathbf{x}}\|^2 + \|\Lambda_2 J_2 \bar{\mathbf{x}}\|^2 \\ &+ \|\Lambda_1 J_1 (\mathbf{x} - \bar{\mathbf{x}})\|^2 + \|\Lambda_2 J_2 (\mathbf{x} - \bar{\mathbf{x}})\|^2 \\ &= (A\bar{\mathbf{x}} + A(\mathbf{x} - \bar{\mathbf{x}}) - \mathbf{b}, A\bar{\mathbf{x}} + A(\mathbf{x} - \bar{\mathbf{x}}) - \mathbf{b}) \\ &+ (\Lambda_1 J_1 \bar{\mathbf{x}} + \Lambda_1 J_1 (\mathbf{x} - \bar{\mathbf{x}}), \Lambda_1 J_1 \bar{\mathbf{x}} + \Lambda_1 J_1 (\mathbf{x} - \bar{\mathbf{x}})) \\ &+ (\Lambda_2 J_2 \bar{\mathbf{x}} + \Lambda_2 J_2 (\mathbf{x} - \bar{\mathbf{x}}), \Lambda_2 J_2 \bar{\mathbf{x}} + \Lambda_2 J_2 (\mathbf{x} - \bar{\mathbf{x}})) \\ &= \|A\bar{\mathbf{x}} - \mathbf{b}\|^2 + \|\Lambda_1 J_1 \bar{\mathbf{x}}\|^2 + \|\Lambda_2 J_2 \bar{\mathbf{x}}\|^2 \\ &+ \|A(\mathbf{x} - \bar{\mathbf{x}})\|^2 + \|\Lambda_1 J_1 (\mathbf{x} - \bar{\mathbf{x}})\|^2 + \|\Lambda_2 J_2 (\mathbf{x} - \bar{\mathbf{x}})\|^2 \\ &+ (A\bar{\mathbf{x}} - \mathbf{b}, A(\mathbf{x} - \bar{\mathbf{x}})) + (A(\mathbf{x} - \bar{\mathbf{x}}), A\bar{\mathbf{x}} - \mathbf{b}) \\ &+ (\Lambda_1 J_1 \bar{\mathbf{x}}, \Lambda_1 J_1 (\mathbf{x} - \bar{\mathbf{x}})) + (\Lambda_1 J_1 (\mathbf{x} - \bar{\mathbf{x}}), \Lambda_1 J_1 \bar{\mathbf{x}}) \\ &+ (\Lambda_2 J_2 \bar{\mathbf{x}}, \Lambda_2 J_2 (\mathbf{x} - \bar{\mathbf{x}})) + (\Lambda_2 J_2 (\mathbf{x} - \bar{\mathbf{x}}), \Lambda_2 J_2 \bar{\mathbf{x}}) \\ &= \|A\bar{\mathbf{x}} - \mathbf{b}\|^2 + \|\Lambda_1 J_1 \bar{\mathbf{x}}\|^2 + \|\Lambda_2 J_2 \bar{\mathbf{x}}\|^2 \\ &+ \|A(\mathbf{x} - \bar{\mathbf{x}})\|^2 + \|\Lambda_1 J_1 (\mathbf{x} - \bar{\mathbf{x}})\|^2 + \|\Lambda_2 J_2 (\mathbf{x} - \bar{\mathbf{x}})\|^2 \\ &+ 2(\mathbf{x} - \bar{\mathbf{x}}, A^T A\bar{\mathbf{x}} - A^T \mathbf{b}) + 2(\mathbf{x} - \bar{\mathbf{x}}, J_1^T \Lambda_1^T \Lambda_1 J_1 \bar{\mathbf{x}}) \\ &+ 2(\mathbf{x} - \bar{\mathbf{x}}, J_2^T \Lambda_2^T \Lambda_2 J_2 \bar{\mathbf{x}}) \\ &= \|A\bar{\mathbf{x}} - \mathbf{b}\|^2 + \|\Lambda_1 J_1 \bar{\mathbf{x}}\|^2 + \|\Lambda_2 J_2 \bar{\mathbf{x}}\|^2 \\ &+ \|A(\mathbf{x} - \bar{\mathbf{x}})\|^2 + \|\Lambda_1 J_1 (\mathbf{x} - \bar{\mathbf{x}})\|^2 + \|\Lambda_2 J_2 (\mathbf{x} - \bar{\mathbf{x}})\|^2 \\ &+ 2(\mathbf{x} - \bar{\mathbf{x}}, A^T A\bar{\mathbf{x}} + J_1^T (\Lambda_1)^2 J_1 \bar{\mathbf{x}} \\ &\quad + J_2^T (\Lambda_2)^2 J_2 \bar{\mathbf{x}} - A^T \mathbf{b}), \end{aligned}$$

where the inner product (\cdot, \cdot) is in the real field. We observe that equation (16) is condition necessary and sufficient for $\bar{\mathbf{x}}$ to minimise the Tikhonov functional. The existence of a unique solution of (16) is due to the non-singularity of the coefficient matrix, which can be easily shown to be a symmetric positive definite matrix and so its minimum eigenvalue is greater than zero. \square

Acknowledgment:

Nadaniela Egidi, Josephin Giacomini and Pierluigi Maponi are members of the Gruppo Nazionale Calcolo Scientifico-Istituto Nazionale di Alta Matematica (GNCS-INdAM).

References:

- [1] Simone Angeloni et al. “Computer Percolation Models for Espresso Coffee: State of the Art, Results and Future Perspectives”. In: *Applied Sciences* 13.4 (2023), p. 2688.
- [2] Yonghui Qiao et al. “Numerical simulation of two-phase non-Newtonian blood flow with fluid-structure interaction in aortic dissection”. In: *Computer methods in biomechanics and biomedical engineering* 22.6 (2019), pp. 620–630.
- [3] Nadaniela Egidi, Josephin Giacomini, and Pierluigi Maponi. “Mathematical model to analyze the flow and heat transfer problem in U-shaped geothermal exchangers”. In: *Applied Mathematical Modelling* 61 (2018), pp. 83–106. DOI: <https://doi.org/10.1016/j.apm.2018.03.024>
- [4] Xiaohua Wu and Parviz Moin. “A direct numerical simulation study on the mean velocity characteristics in turbulent pipe flow”. In: *Journal of Fluid Mechanics* 608 (2008), pp. 81–112.
- [5] Kerstin Avila et al. “The Onset of Turbulence in Pipe Flow”. In: *Science* 333 (2011), pp. 192–196.
- [6] L Hadj-Taieb and E Hadj-Taieb. “Numerical simulation of transient flows in viscoelastic pipes with vapour cavitation”. In: *International Journal of Modelling and Simulation* 29.2 (2009), pp. 206–213
- [7] Alexandre K Soares, Dídia IC Covas, and Nelson JG Carriço. “Transient vaporous cavitation in viscoelastic pipes”. In: *Journal of Hydraulic Research* 50.2 (2012), pp. 228–235
- [8] Lin Wu, Kui-sheng Chen, and Yuan Guo. “Research on cavitation phenomena in pilot stage of jet pipe servo-valve with a rectangular nozzle based on large-eddy simulations”. In: *AIP Advances* 9.2 (2019), p. 025109.
- [9] David N. Ku. “Blood flow in arteries”. In: *Annual Review of Fluid Mechanics* 29 (1997), pp. 399–434.
- [10] S Bandyopadhyay and GC Layek. “Study of magnetohydrodynamic pulsatile flow in a constricted channel”. In: *Communications in Nonlinear Science and Numerical Simulation* 17.6 (2012), pp. 2434–2446.
- [11] João A Isler, Rafael S Gioria, and Bruno S Carmo. “Pulsatile flow in a constricted channel: flow behaviour and equilibrium states”. In: *Journal of Fluid Mechanics* 866 (2019).
- [12] AE Catania, A Ferrari, and E Spessa. “Temperature variations in the simulation of high-pressure injection-system transient flows under cavitation”. In: *International Journal of Heat and Mass Transfer* 51.7-8 (2008), pp. 2090–2107.

- [13] Huan-Feng Duan et al. "Influence of nonlinear turbulent friction on the system frequency response in transient pipe flow modelling and analysis". In: *Journal of Hydraulic Research* 56.4 (2018), pp. 451–463.
- [14] HongGuang Sun et al. "A space fractional constitutive equation model for non-Newtonian fluid flow". In: *Communications in Nonlinear Science and Numerical Simulation* 62 (2018), pp. 409–417.
- [15] Mark Orazem. *Underground pipeline corrosion*. 63. Elsevier, 2014.
- [16] Umangkumar Bharatiya et al. "Effect of corrosion on crude oil and natural gas pipeline with emphasis on prevention by ecofriendly corrosion inhibitors: a comprehensive review". In: *Journal of Bio-and Tribo-Corrosion* 5.2 (2019), pp. 1–12.
- [17] EV Moskvicheva, PA Sidyakin, and DV Shitov. "Method of corrosion prevention in steel pressure pipelines in sewerage systems". In: *Procedia Engineering* 150 (2016), pp. 2381–2386.
- [18] Mehdi Davoudi et al. "Chemical injection policy for internal corrosion prevention of South Pars sea-pipeline: A case study". In: *Journal of Natural Gas Science and Engineering* 21 (2014), pp. 592–599.
- [19] Vikas Kannojiya, Arup Kumar Das, and Prasanta Kumar Das. "Simulation of blood as fluid: A review from rheological aspects". In: *IEEE Reviews in Biomedical Engineering* 14 (2020), pp. 327–341.
- [20] Hamidreza Gharahi et al. "Computational fluid dynamic simulation of human carotid artery bifurcation based on anatomy and volumetric blood flow rate measured with magnetic resonance imaging". In: *International journal of advances in engineering sciences and applied mathematics* 8.1 (2016), pp. 46–60.
- [21] Josephin Giacomini et al. "Testing a model of flow and heat transfer for u-shaped geothermal exchangers". In: *Adv. Model. Anal. A* 55.3 (2018), pp. 151–157.
- [22] Cristina Sàez Blázquez et al. "Efficiency Analysis of the Main Components of a Vertical Closed-Loop System in a Borehole Heat Exchanger". In: *Energies* 10.2 (Feb. 2017), p. 201. DOI: 10.3390/en10020201.
- [23] Nadaniela Egidi, Josephin Giacomini, and Pierluigi Maponi. "Inverse heat conduction to model and optimise a geothermal field". In: *Journal of Computational and Applied Mathematics* 423 (2023), p. 114957.
- [24] Peter Bayer, Michael de Paly, and Marcus Beck. "Strategic optimization of borehole heat exchanger field for seasonal geothermal heating and cooling". In: *Applied Energy* 136 (2014), pp. 445–453.
- [25] Enzo Zanchini, Stefano Lazzari, and Antonella Priarone. "Long-term performance of large borehole heat exchanger fields with unbalanced seasonal loads and groundwater flow". In: *Energy* 38 (2012), pp. 66–77.
- [26] C. D. Argyropoulos and N. C. Markatos. "Recent advances on the numerical modelling of turbulent flows". In: *Applied Mathematical Modelling* 39 (2015), pp. 693–732.
- [27] S. Vijiapurapu and J. Cui. "Performance of turbulence models for flows through rough pipes". In: *Applied Mathematical Modelling* 34 (2010), pp. 1458–1466.
- [28] R. Friedrich et al. "Direct numerical simulation of incompressible turbulent flows". In: *Computers & Fluids* 30 (2001), pp. 555–579.
- [29] Nilanjan Chakraborty, E Mastorakos, and RS Cant. "Effects of turbulence on spark ignition in inhomogeneous mixtures: a direct numerical simulation (DNS) study". In: *Combustion science and technology* 179.1-2 (2007), pp. 293–317.
- [30] Gary N Coleman and Richard D Sandberg. *A primer on direct numerical simulation of turbulence-methods, procedures and guidelines*. Tech. rep. SO17 1BJ, UK: University of Southampton, 2010.
- [31] Lin Zhang et al. "A stability condition for turbulence model: From EMMS model to EMMS-based turbulence model". In: *Particuology* 16 (2014), pp. 142–154.
- [32] Josephin Giacomini. "RBFs preconditioning via Fourier decomposition method". In: *American Institute of Physics Conference Series*. Vol. 3094. 1. 2024, p. 320005.

- [33] D. Colton and R. Kress. *Inverse Acoustic and Electromagnetic Scattering Theory*. Springer-Verlag, 1998.
- [34] Alfio Quarteroni and Alberto Valli. *Numerical Approximation of Partial Differential Equations*. Springer, 1994.
- [35] Roger Temam. *Navier-Stokes equations*. North-Holland Publishing Company, 1977.
- [36] Charles Hirsch. *Numerical Computation of Internal & External Flows*. Second. Butterworth-Heinemann, 2007.
- [37] Andreas Kirsch et al. *An introduction to the mathematical theory of inverse problems*. Vol. 120. Springer, 2011.
- [38] Vladimir Alekseevich Morozov. *Regularization Methods for Ill-Posed Problems*. CRC Press, 1993.
- [39] C. Cuvelier, A. Segal, and A.A. Van Steenhoven. *Finite Element Methods and Navier Stokes equations*. D. Reidel Publishing Company, 1977.
- [40] A. Bejan. *Convection Heat Transfer*. John Wiley & Sons, Inc., 2004.
- [41] J.H. Ferziger and M. Perić. *Computational Methods for Fluid Dynamics*. Springer, 2002.
- [42] Yunus A. Çengel and Jhon M. Cimbala. *Fluid Mechanics: Fundamentals and Applications*. Third. McGraw-Hill, 2014.
- [43] Len G Margolin. “The reality of artificial viscosity”. In: *Shock Waves* 29.1 (2019), pp. 27–35.

Contribution of Individual Authors to the Creation of a Scientific Article (Ghostwriting Policy)

The authors equally contributed in the present research, at all stages from the formulation of the problem to the final findings and solution.

Sources of Funding for Research Presented in a Scientific Article or Scientific Article Itself

This research received partial funding from the Unione Europea - FSE, Pon Ricerca e Innovazione 2014-2020 (Decreto Ministeriale 1062 - 10/08/2021).

Conflicts of Interest

The authors have no conflicts of interest to declare that are relevant to the content of this article.

Creative Commons Attribution License 4.0 (Attribution 4.0 International , CC BY 4.0)

This article is published under the terms of the Creative Commons Attribution License 4.0

https://creativecommons.org/licenses/by/4.0/deed.en_US